PHYSICAL REVIEW B **86**, 174112 (2012)

Stress-driven island growth on top of nanowires

Frank Glas*
CNRS - Laboratoire de Photonique et de Nanostructures, Route de Nozay, 91460 Marcoussis, France

Bruno Daudin
CEA-CNRS-UJF Group Nanophysique et Semiconducteurs, CEA, INAC, 17 rue des Martyrs, 38054 Grenoble, France
(Received 24 August 2012; published 16 November 2012)

We model the coherent deposition of a mismatched material on the top facet of a nanowire and investigate the possible formation of a cylindrical island that is narrower than the nanowire stem. We calculate the elastic relaxation and the total energy of the system and determine the optimal shape of the deposit as a function of misfit, nanowire radius, and deposit thickness. If the values of any two of these parameters are set, then there is a critical value of the third one above which the formation of a genuine island that is narrower than the stem is favored compared to that of a disk of equal volume covering entirely the top facet. These critical values are easily accessible in current nanowire systems, and we predict that islanding can lead to a large reduction of the total energy. We discuss the similarities and differences between the present effect and the standard Volmer-Weber and Stranski-Krastanow growth modes. For semiconductor nanowires, islanding is likely to occur primarily in the case of catalyst-free growth. We argue that it might already have been observed in heterostructures of nanowires of group-III nitrides.

DOI: 10.1103/PhysRevB.86.174112 PACS number(s): 62.23.Hj, 81.07.Ta, 62.20.−x, 81.10.Aj

I. INTRODUCTION

It is commonly observed that a mismatched material deposited epitaxially on a bulk planar substrate tends to grow as islands rather than as a uniformly thick layer [hereafter termed two-dimensional (2D) layer]. There are two variants of this growth mode, known as Volmer-Weber (VW) and Stranski-Krastanow (SK), which differ by the absence (VW) or presence (SK) of a thin wetting layer on the substrate. In both cases, the driving force for the nucleation of the coherent islands is the reduction of elastic energy afforded by strain relaxation at the free lateral surfaces of the islands and strain partition between islands and substrate. Observed for more than 25 years,[1] the SK growth of semiconductors has spurred the spectacular development of quantum dot (QD) nanostructures.

Inserting QDs in semiconductor nanowires (NWs) offers an attractive alternative to growing them on planar substrates, with applications ranging from tunneling devices[2] to light-emitting diodes[3] and sources of single or entangled photons.[4–8] NWs then constitute very narrow *effective* substrates that present several advantages. In the planar case, the QDs tend to nucleate randomly on the surface (or even, for group-III nitrides, in the vicinity of threading dislocations)[9] and the dispersions of their shapes and dimensions may constitute a major drawback. In the NW case, the location of the QD is predetermined by that of the NW. Ordered arrays of NWs can be grown by using lithography methods in the vapor-liquid-solid (VLS) mode (by patterning the catalyst droplets)[10] as well as in the catalyst-free mode.[11] Moreover, the dimensions of the QD are controlled by the NW diameter and the growth time. Indeed, when one forms an axial heterostructure in a NW, the deposit usually adopts the diameter of the NW stem. There may be two reasons for this. The first is specific to VLS growth, where each new monolayer (ML) tends to nucleate at the triple phase line[12,13] or in its vicinity[14,15] before rapidly spreading over the whole top facet of the NW.[16,17] The second reason is related to misfit. At variance with deposition on a laterally infinite substrate, elastic relaxation at the NW sidewalls is very effective[18–21] so that there seems to be little driving force for forming an island rather than a layer covering entirely the top facet of the NW (later termed *disk*). In these conditions, the insertion of a QD in a NW starts with the deposition of a layer which adopts the same diameter as the NW, with lateral confinement being provided by the subsequent growth of a shell around the whole structure.[22,23]

There are indeed many reports of QDs grown in a non-VLS, catalyst-free fashion that adopt the diameter of the underlying NW.[24–26] However, several groups have also observed that a nominally homogeneous *alloy* deposited on a misfitting NW stem may spontaneously adopt a core-shell structure.[27–29] We may imagine two scenarios leading to such a structure (Fig. 1): either the deposit grows layer by layer on the whole top facet, but each ML is radially inhomogeneous [Fig. 1(a)], or else the process starts with the formation of an island narrower than the NW stem, which is capped laterally by another material during the subsequent stages of growth [Fig. 1(b)]. Although these scenarios might be distinguished by observing the early stages of deposition, this does not seem to have been done so far. For the reasons mentioned earlier, we expect such processes to occur primarily, if at all, for catalyst-free growth, and the observations listed above[27–29] actually pertain to the catalyst-free growth of NWs of group-III nitrides.

Niu *et al.*[30] recently addressed the first scenario [Fig. 1(a)] and showed that it can indeed happen in certain growth conditions, but of course only for alloys. Here, we explore the first stage of the second possible mode of spontaneous QD formation [Fig. 1(b)], which is the only one conceivable for elemental or binary compound semiconductors. Namely, we study if the growth of a homogeneous mismatched material on top of a NW might lead to the spontaneous formation of islands narrower than the NW, a mechanism that would be

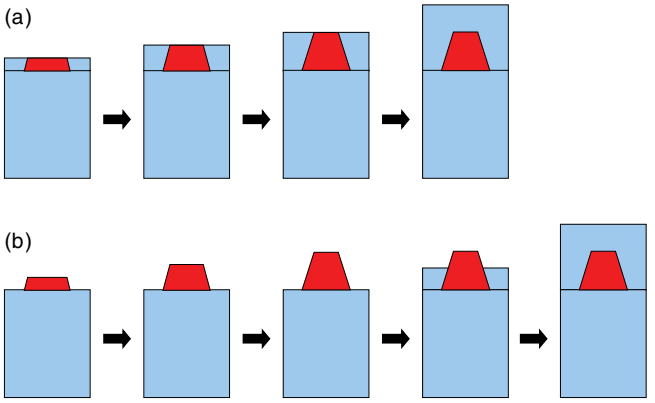

FIG. 1. (Color online) Two scenarios for the spontaneous formation of a quantum dot on top of a NW. (a) Continuous growth of radially inhomogeneous alloy monolayers. (b) Island growth followed by conformal shell embedding.

akin to VW or SK growth, despite the easy stress relaxation at the NW free surfaces. In the present work, we only treat the energetics of the problem, not its kinetics. Note that we consider the formation of misfitting islands on the *top facet* of the NW. This differs totally from the formation of islands or corrugations on the *sidewalls* of the NW, a problem that several groups have already investigated experimentally[31–33] and theoretically.[34]

II. MODEL AND CALCULATIONS

A. Model

As a first approximation, and in order to keep to a minimum the parameters defining the system while still capturing the basic physical ingredients of the problem, we consider an axisymmetric structure consisting of a long cylindrical NW stem of radius R_{NW} topped by a misfitting axial cylindrical island of radius $R \leqslant R_{NW}$ and height H [Fig. 2(a)]. We assume that the island is homogeneous (even in the case of an alloy) and that lattice accommodation at the NW/island interface is coherent (no extended defect is present).

We calculate the increase W_t of the total energy of the system upon forming the island as the sum of the elastic energy W_e generated by the coherent relaxation of the whole system and of an energy W_s associated to surfaces, and possibly

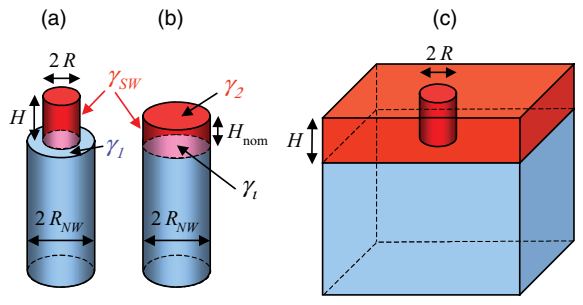

FIG. 2. (Color online) Schematics of islands of equal volumes covering the top facet of the nanowire either (a) partly or (b) fully (disk); (c) equivalent volume as part of a 2D layer grown on a bulk substrate.

interfaces, created or destroyed upon island formation. To calculate the elastic energy, we assume that the NW and the island are isotropically elastic materials, with identical Young moduli E and Poisson ratios ν. The relative mismatch is specified by a single quantity ϵ_0 (the stress-free strain). As regards the surface energy (the components of which are indicated in Fig. 2), we consider two cases. Either we limit ourselves to that of the island sidewalls, $W_{SW} = 2\pi RH\gamma_{SW}$, with γ_{SW} the areal energy of the sidewalls [Eq. (1a)], or, in addition [Eq. (1b)], we also consider the energies associated with the formation of the top surface of the island (areal energy γ_2) and of the NW/island interface (γ_i) and with the disappearance of this part of the top surface of the NW stem that becomes occupied by the island (γ_1). Hence,

$$W_t = W_e + 2\pi RH\gamma_{SW} \quad \text{(case 1)} \quad \text{(1a)}$$

$$\text{or} \quad W_t = W_e + 2\pi RH\gamma_{SW} + \pi R^2\Delta\gamma \quad \text{(case 2)} \quad \text{(1b)}$$

where $\Delta\gamma = \gamma_2 + \gamma_i - \gamma_1$.

Our aim is to develop a generic model not tied to any specific material system, to determine general trends as a function of system geometry and misfit, and to find possible critical values of these parameters for islanding. Hence, we allow the system dimensions, in particular the island thickness H, to vary *continuously* and to take small values. It should, however, be borne in mind that in any particular semiconductor, a disk or an island is made of an integer number of MLs, with the minimum thickness being one ML.

B. Elastic energy

In the framework of linear isotropic elasticity, for given elastic constants, the strain field depends only on the relative dimensions of the system and scales with ϵ_0. As regards the elastic constants, the elastic energy scales with E but depends on ν in a nontrivial fashion, albeit rather weakly. Hence, for a given Poisson ratio, in order to get the full variations of W_e with system geometry and mismatch, it suffices to perform calculations for a single mismatch and a single NW radius and to vary *independently* the radius and height of the island:

$$W_e(R_{NW}, R, H; \epsilon_0, E, \nu) = E\epsilon_0^2 \left(\frac{R_{NW}}{R_0}\right)^3 w_e\left(\frac{R_0}{R_{NW}}R, \frac{R_0}{R_{NW}}H; \nu\right), \quad (2)$$

where $w_e(r,h;\nu)$ is the reduced elastic energy calculated for an island of radius r and height h sitting on top of a NW of arbitrary unit radius R_0, with $\epsilon_0 = 1$ and $E = 1$.

In practice, for want of an analytical solution to the elastic problem, we calculate numerically the strain state and the reduced elastic energy w_e for a given value of the NW radius R_0 and for a wide range of discrete values of island radius $r \leqslant R_0$ and height h, by using the COMSOL software.[35] We then fit w_e to a continuous function of r and h. As in the case of axial (disk) heterostructures ($r = R_0$),[19] the fitting function must satisfy some constraints due to the following asymptotic limits:

(i) For any given r, when $h \to 0$, the lateral extension of the deposit becomes effectively infinite so that w_e tends to the energy of the same volume of deposit cut in a 2D layer coherently deposited on a bulk substrate with identical elastic constants[19] [Fig. 2(c)], namely, $w_{2D}(r,h;\nu) =$

$W_{2D}(r,h;\epsilon_0=1,E=1,\nu)$, with $W_{2D}(r,h;\epsilon_0,E,\nu) = \pi r^2 h E \epsilon_0^2/(1-\nu)$. Hence the ratio

$$f_\nu(r,h) = w_e(r,h;\nu)/w_{2D}(r,h;\nu) \tag{3}$$

tends to 1 when $h \to 0$.

(ii) Because of strain relaxation at their sidewalls, tall islands are substantially strained only over a height of the order of their radius.[19] Hence, when $h \to \infty$, w_e tends to an r-dependent constant whereas w_{2D} scales with $r^2 h$ and, for r given, f_ν varies asymptotically as $1/h$.

We find that the following function, which satisfies constraints (i) and (ii), satisfactorily fits function f_ν [defined by Eq. (3)] at fixed r:

$$\varphi_\nu(r,h) = \frac{1+t_1 h \exp[-t_3 h]}{1+t_2 h}. \tag{4}$$

In Eq. (4), t_i $(i=1,2,3)$ are r-dependent parameters which are themselves fitted by functions:

$$t_i(r) = \sum_{j=-1}^{4} A_{ij} r^j. \tag{5}$$

We have derived such fitting functions by performing numerical calculations of w_e for more than 150 (r,h) couples (spanning the ranges $0.04 \leqslant r/R_0 \leqslant 1$ and $0.01 \leqslant h/R_0 \leqslant 4$) and for three values of the Poisson ratio, namely, $\nu = 0.25$, 0.33, and 0.41. The corresponding parameters are given in Table I. The best fit of the energy as a function of island dimensions was found independently for each value of ν. This produced values of the A_{ij} parameters which are not smooth functions of ν. However, the A_{ij} parameters, taken individually, have no physical meaning. Energy w_e and function f, on the other hand, vary smoothly with ν, when all other parameters (and, in particular, the dimensions) are fixed. Hence, values of f_ν for other values of ν can be obtained by interpolating f_ν (and not the fitting parameters A_{ij}).

The variations of the ratio f_ν for $0 \leqslant h/R_0 \leqslant 4$ and the quality of the fits are illustrated in Fig. 3 for a large range of values of the normalized island radius r/R_0. In the case $r = R_0$, Eqs. (4) and (5) provide fits refined from those given in Ref. 19.

The general trends are the following. At fixed island radius r, f_ν decreases when island height h increases. However, at fixed island height, the variations of f_ν are more complex: whereas f_ν increases with small radii, it varies little and nonmonotonically with r for $r \gtrsim R_0/2$. This manifests the intricate interplay of elastic relaxation at the lateral free surfaces of the island and NW stem when these have similar radii.

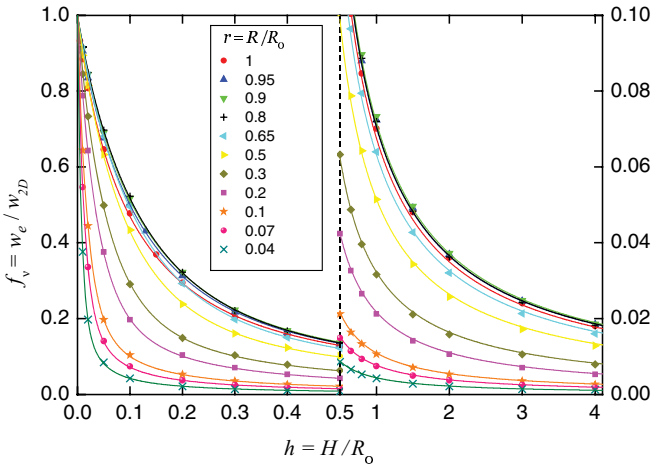

FIG. 3. (Color online) Variations of the ratio of the elastic energy stored in the system made of a misfitting island coherently deposited on a NW stem [Fig. 2(a)] to that stored in a volume equal to the island, cut in a 2D layer [Fig. 2(c)], with the layer/substrate and island/NW misfits being equal. Variations are given as a function of island height h for various values of the island radius r, with h and r in units of NW radius R_0, and $\nu = 0.33$. Each symbol represents a numerical calculation made for a given island geometry. The curves are fits of these data with functions φ_ν given by Eqs. (4) and (5). Since w_e gets smaller and varies more slowly at high h, the graph is divided in two halves for the sake of visibility: starting from $h = 0.5$, the horizontal scale is contracted by a factor of 7.2 and the vertical scale is expanded by a factor of 10 (right axis).

C. Energy minimization

Once the fitting functions are determined, we obtain an analytical expression for the total energy $W_t(R_{NW},R,H;\epsilon_0,E,\nu)$ as a function of dimensions, misfit, and elastic constants by adding the elastic energy given by Eqs. (2)–(5) to the surface and possibly interface energies, according to Eq. (1a) or (1b). We then find the *optimal* aspect ratio of the island *for a given total deposit volume* V, i.e., the radius-height couple $(R_{\rm opt},H_{\rm opt})$ that minimizes total energy W_t under the constraint $\pi R^2 H = V$. This minimization is performed for a wide range of NW radii R_{NW}, deposit volumes V, and relative lattice mismatches ϵ_0. For each set of these parameters, the minimum energy $W_{\rm opt}$ is then compared to the total energy $W_{\rm disk} = W_t(R_{NW},R_{NW},H_{\rm nom};\epsilon_0,E,\nu)$ for a deposit of equal volume and equal misfit wholly covering the top facet of the NW, i.e., a disk of nominal thickness $H_{\rm nom} = \pi^{-1} V/R_{NW}^2$

TABLE I. Parameters A_{ij} for the calculation of the elastic energy according to Eqs. (2)–(5).

	$\nu = 0.25$			$\nu = 0.33$			$\nu = 0.41$		
j	$i=1$	$i=2$	$i=3$	$i=1$	$i=2$	$i=3$	$i=1$	$i=2$	$i=3$
−1	4.49588	8.57313	6.50236	4.88471	8.96602	6.8399	4.65864	9.31206	6.69716
0	−4.47476	2.05094	−6.98281	−12.55246	1.92076	−12.72769	−7.58291	1.85064	−5.0962
1	14.57256	−16.75704	26.48042	65.82582	−17.5834	70.75007	29.99425	−16.21396	14.21671
2	−33.09847	50.56185	−38.63564	−165.45649	55.6273	−169.9425	−65.97962	50.81011	−9.15628
3	44.65054	−61.46454	22.1264	190.63404	−69.68977	182.91743	77.13609	−63.82867	−7.27382
4	−23.10718	30.38787	−0.43759	−80.58307	34.52705	−69.51665	−35.30009	32.13003	9.81956

[Fig. 2(b)]. When $W_{\rm opt}/W_{\rm disk} < 1$, the island is preferred to the disk, whereas the disk is favored when $W_{\rm opt}/W_{\rm disk} = 1$.

In Secs. III and IV, we investigate the system behavior under various hypotheses. In Sec. III, the only surface energy considered is that of the sidewalls [Eq. (1a)]. There are several reasons for doing so. In general, the interface energy is only a minor contribution to the total energy.[36,37] This might not be the case for the energies of the top surfaces of the NW and island. However, only their difference appears in the calculation. Moreover, in the usual case of the {0001} wurtzite or {111} sphalerite polar surfaces, these quantities are not well defined since only a pair of different such surfaces can be created by cleavage. Only differences of such energies for the same material are defined, and they also vary with the chemical potentials of the group-III and group-V species in the vapor phase[38] and with strain.[39] Nevertheless, in Sec. IV, we will discuss in a general fashion how the conclusions of Sec. III are modified for either positive or negative values of $\Delta\gamma$.

III. RESULTS WITH ELASTIC AND SIDEWALL SURFACE ENERGIES ONLY

In the following, we discuss the preference for forming an island rather than a disk (Secs. III A and III B) and the optimal aspect ratio of the island (Sec. III C) as a function of misfit and geometry. We find that these depend little on the value of the Poisson ratio ν. We illustrate our results for $\nu = 0.33$. We take $E = 3.24 \times 10^{11}$ Pa and $\gamma_{SW} = 1.8\ {\rm J/m^2}$. These values closely approximate those of NWs of (In,Ga)N alloys with moderate In concentrations, growing along $(000\bar{1})$ with $\{10\bar{1}0\}$ side facets.[39–41]

In the present section, in addition to the elastic energy, we only take into account the surface energy of the sidewalls [Eq. (1a)]. Quite generally, at fixed deposit volume V, when the island radius R decreases from its maximum value R_{NW}, the elastic energy decreases (recall that the strained volume varies roughly as R^3 at low R), but at the same time the sidewall energy, which scales with the sidewall area $2V/R$, increases. Whether or not a minimum of the total energy will occur at some radius $R < R_{NW}$ depends on the relative weights of the elastic and sidewall energies (see Sec. III B for more details). This is already the case for growth on a 2D substrate, but here the elastic energy is deeply modified by the proximity of the NW sidewalls.

A. Critical misfit for island formation

Figures 4 and 5 show the variations of the ratio $W_{\rm opt}/W_{\rm disk}$ (defined in Sec. II C) as a function of NW radius R_{NW} and nominal deposit thickness $H_{\rm nom}$. In Figs. 4 and 5, the various maps correspond to three different values of misfit ϵ_0, and we consider NW radii up to 50 nm and deposit thicknesses up to 2.7 nm. Note that the optimal configuration (disk or island, and, in the latter case, optimal aspect ratio of the island) is found for a given deposit volume V, whereas the quantity along the y axis in Figs. 4 and 5 is $H_{\rm nom} = \pi^{-1}V/R_{NW}^2$ (see Sec. II C). This choice is made in order to facilitate comparison with experiments, where the amount deposited per unit area is a privileged control parameter. For the same reason, we express $H_{\rm nom}$ in terms of MLs of thickness 0.27 nm; this

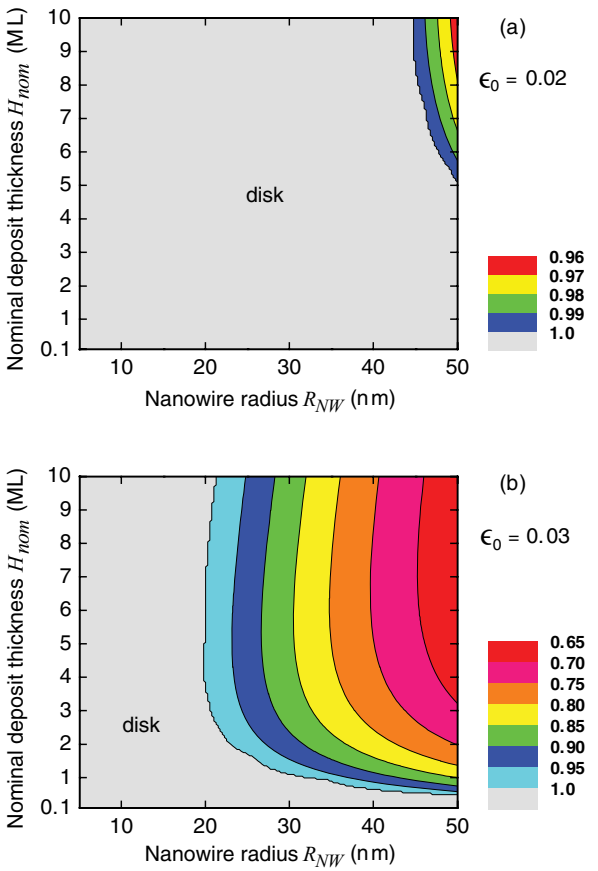

FIG. 4. (Color online) Map of the variations as a function of NW radius and nominal deposit thickness of the ratio $W_{\rm opt}/W_{\rm disk}$ of the minimum energy of the system (at given deposit volume) to its energy in the disk configuration. The nominal deposit thickness is expressed in monolayers of thickness 0.27 nm. The misfit ϵ_0 of the deposit with respect to the NW is (a) 2% or (b) 3%. The gray zones at left and bottom are where the disk is favored (ratio equal to 1), whereas island formation is preferred in the colored areas. Material parameters: $\nu = 0.33$, $E = 3.24 \times 10^{11}$ Pa, $\gamma_{SW} = 1.8\ {\rm J/m^2}$.

value is arbitrary but close to the ML thickness in a standard $\langle 0001\rangle$ direction for the wurtzite nitrides or $\langle 111\rangle$ for the cubic semiconductors. Nevertheless, as mentioned earlier, our continuum approach allows us to consider deposits thinner than 0.27 nm (1 ML here), which is useful to clarify effects occurring at low deposit thickness (Sec. III B) and would be necessary for other materials with lower ML thickness (in practice, a deposit may of course have an *average* thickness below 1 ML and be made of discontinuous patches of 1 ML thickness, but our model does not handle this case).

Each map in Figs. 4 and 5 may be viewed as a stability diagram where the gray area at left and bottom corresponds to a stable disk and the colored bands correspond to a disk unstable against its transformation into an island. The aspect ratios of the optimal islands, which realize the minimum energies plotted in Figs. 4 and 5, will be discussed in Sec. III C.

For the lowest misfit considered [$\epsilon_0 = 2\%$; Fig. 4(a)], there is very little tendency to island formation. We observe a reduction of total energy for the island configuration only for $R_{NW} > 45$ nm and $H_{\rm nom} > 5$ MLs, and at most by a few percent. However, for $\epsilon_0 = 3\%$ [Fig. 4(b)], it becomes

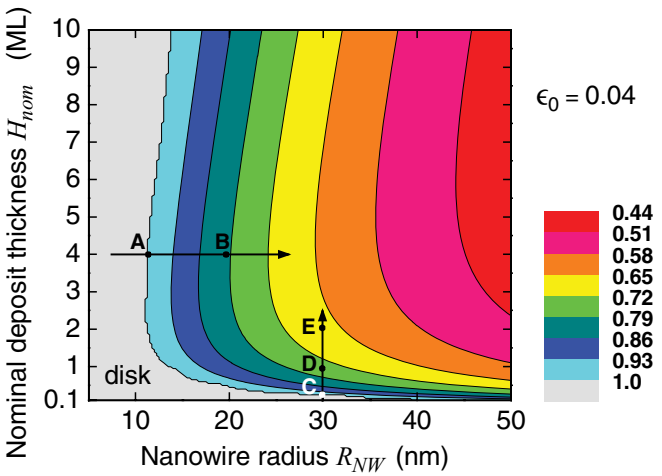

FIG. 5. (Color online) Same as Fig. 4 for $\epsilon_0 = 4\%$. The arrows illustrate the existence of a deposit-thickness-dependent critical NW radius and a NW-radius-dependent critical deposit thickness.

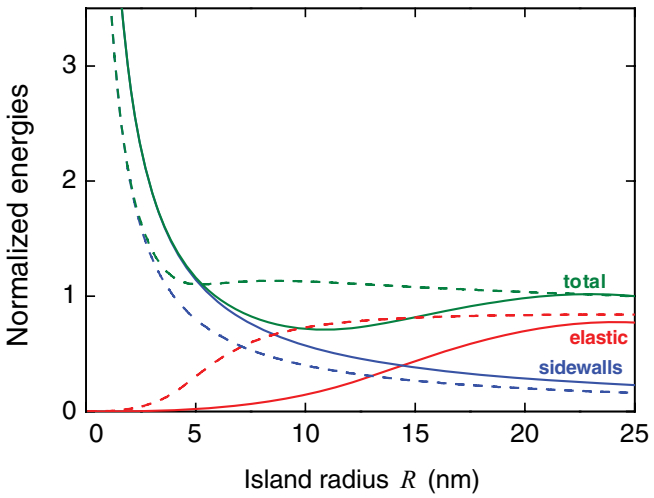

FIG. 6. (Color online) Variation with island radius, at fixed island volume V and for a given NW radius $R_{NW} = 25$ nm, of the elastic (red curves), sidewall (blue curves), and total (green curves) energies. Full and dashed curves correspond, respectively, to deposit thicknesses of 5 and 0.2 MLs (at full NW radius). The energies are normalized to the total energy of the disk with the same volume. Material parameters as in Figs. 4 and 5; $\epsilon_0 = 4\%$.

energetically favorable to form islands at a much lower NW radius (about 20 nm) and deposit thickness (about 1 ML). Moreover, the reduction of energy may be substantial, e.g., up to about a third of the energy of the disk configuration in the parameter ranges considered. This tendency is confirmed in the case $\epsilon_0 = 4\%$ (Fig. 5). Then, there is a preference for island over disk as soon as $R_{NW} > 10$ nm; for higher radii, the reduction of energy may be larger than 50%.

For a given (NW radius, deposit thickness) couple, the relative energy reduction increases with misfit. For each couple (at least in a large domain), there is a critical misfit above which island formation becomes favorable, as expected from the increased relative weight of the elastic energy with misfit [Eq. (2)].

B. Critical NW radius and critical deposit thickness

In addition to the misfit, the geometrical parameters that define the system exhibit critical values. We discuss this in the case $\epsilon_0 = 4\%$ (Fig. 5), but our conclusions remain valid for other misfits.

We first observe that for each nominal deposit thickness, there is a critical NW radius above which the island configuration becomes favorable. As illustrated in Fig. 5 for a deposit of 4 MLs (horizontal arrow), we may adopt various criteria for defining its value, such as the radius where, upon forming the island, there is a vanishing gain in energy (point A) or else a given relative gain (e.g., 20% at point B). However, whatever the criterion and except at very small deposited thickness (see below), this NW radius depends little on this thickness (the boundaries in Fig. 5 are nearly vertical) and can thus rightly be taken as a critical radius for the morphological transition. For instance, using the first criterion, it only varies by 2.5 nm for nominal deposits ranging between 1 and 10 MLs.

The picture is quite different at very low deposit thicknesses (recall that we consider arbitrarily thin deposits). Then, the disk is systematically favored and the critical NW radius varies rapidly with deposit thickness, as witnessed by the shallowly sloped boundaries in Figs. 4(b) and 5. This can be understood by considering separately the variations of the elastic and sidewall energies as a function of island radius, at fixed deposit volume and for a given NW radius (Fig. 6). For all but the thinnest deposits (full lines in Fig. 6), when the island radius is reduced (starting from the NW radius), considerable elastic relaxation takes place. In a range of island radii, this overcomes the increase of sidewall energy, so that a more or less pronounced minimum of the total energy occurs at some radius, which defines the optimal island (Sec. II C). On the contrary, for a low deposit thickness (dashed lines in Fig. 6), the elastic energy of the system remains approximately constant for a wide range of island radii because the elastic state of the island remains very close to that of a 2D layer. When the island radius is reduced enough for elastic relaxation to become substantial (say, to about a third of the NW radius in the example of Fig. 6), the sidewall energy has increased too much to be compensated by this reduction, and no minimum of the total energy occurs (as seen in Fig. 6, a weak local minimum may still occur, but this is not the absolute minimum, which is found at $R = R_{NW}$).

Hence, at a given NW radius, a transition from disk to island occurs when the deposit thickness increases, and this transition is very sharp. For instance, for $R_{NW} = 30$ nm (vertical arrow in Fig. 5), there is no gain in energy up to 0.25 ML deposited (point C), but the gain in forming an island is already 1/4 of the disk energy at 1 ML (point D) and 1/3 at 2.1 MLs (point E). The same holds for $\epsilon_0 = 3\%$, where, for the same radius, there is no gain up to 1.15 ML and a 10% gain at 2.4 MLs [Fig. 4(b)]. This is very reminiscent of the SK growth mode of mismatched epitaxial layers on bulk substrates whereby, as the deposit thickness increases, a sharp transition occurs between a continuous 2D layer of uniform thickness and islands resting on the remains of this layer (the wetting layer). There are, however, differences with the standard SK

transition. In particular, our simple model does not account for a transition whereby the disk would transform partly into a pseudo-2D layer covering entirely the top facet (a thinner disk) and partly into an island resting on top of it (which is, however, not likely since the formation of a wetting layer would reduce the effective volume of the island and thus increase the total energy). Moreover, we assumed that the energies of the top facets of the NW stem and deposit are equal, whereas a difference in substrate and deposit surface energies plays a crucial part in the SK transition of semiconductor heterostructures. This will be discussed in Sec. IV. Finally, for large NW radii, i.e., precisely when we approach growth on a bulk substrate, the deposit thickness up to which the disk is favored tends to zero [Figs. 4(b) and 5] and not to the finite thickness that characterizes the standard SK transition, as opposed to the VW transition.

C. Optimal aspect ratio of the island

The optimal aspect ratio of the deposit also exhibits sharp transitions when the system parameters are modified. This is demonstrated in Fig. 7 where, again for $\epsilon_0 = 4\%$, we map the radius R_{opt} of the optimal island, as defined in Sec. II C, normalized by the NW radius. Indeed, when the NW radius is increased above the critical radius at fixed deposit thickness, the island very quickly adopts an aspect ratio notably different from that of the disk. For instance, for a deposit of 4 MLs, the transition between the disk ($R = R_{NW}$) and an island having a radius equal to only $2R_{NW}/3$ occurs for an increase of R_{NW} of only 0.25 nm. Of course, this transition is not likely to be observed in practice, unless the NW radius increases by radial growth as well as axial growth. On the other hand, the increase of the deposit thickness at a constant NW radius corresponds to a standard growth sequence. And this also gives rise to a sharp transition between the disk and an island notably narrower than the NW, all the more so that the NW radius is large.

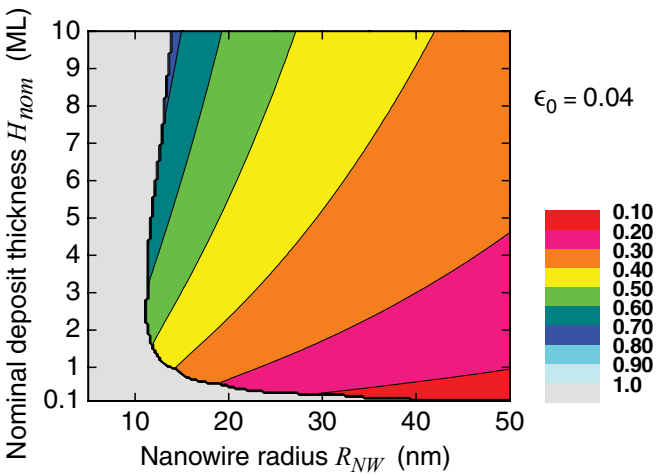

FIG. 7. (Color online) Map of the variations as a function of NW radius and deposit thickness of the radius of the optimal island. The radius is expressed in units of NW radius. Material parameters as in Fig. 5.

IV. RESULTS WITH ALL SURFACE ENERGIES INCLUDED

In this section, we discuss how the conclusions of Sec. III are modified by including the difference in surface energies between the top facets of the NW and island. In Fig. 8, we retain the same parameters as in Fig. 5, but we now consider values of $\Delta\gamma$ equal to $\pm 10\%$ of the sidewall areal energy, instead of $\Delta\gamma = 0$.

When $\Delta\gamma < 0$ [Fig. 8(a)], islands with wide top facets, and ultimately disks, are favored. Consequently, the disk/island boundary and the lines of the equal $W_{\text{opt}}/W_{\text{disk}}$ ratio shift towards higher values of the NW radius with respect to the case $\Delta\gamma = 0$. However, although the domain of preference for the disk with respect to the true island is enlarged, the general shape of the diagram remains unaltered. In particular, there still exist critical radii and critical thicknesses, albeit larger than when $\Delta\gamma = 0$.

The modifications might appear larger in the case $\Delta\gamma > 0$ [Fig. 8(b)]. However, except for the thinnest deposits, the main modification of the stability diagram is that the disk/island boundary and the lines of equal $W_{\text{opt}}/W_{\text{disk}}$ are displaced

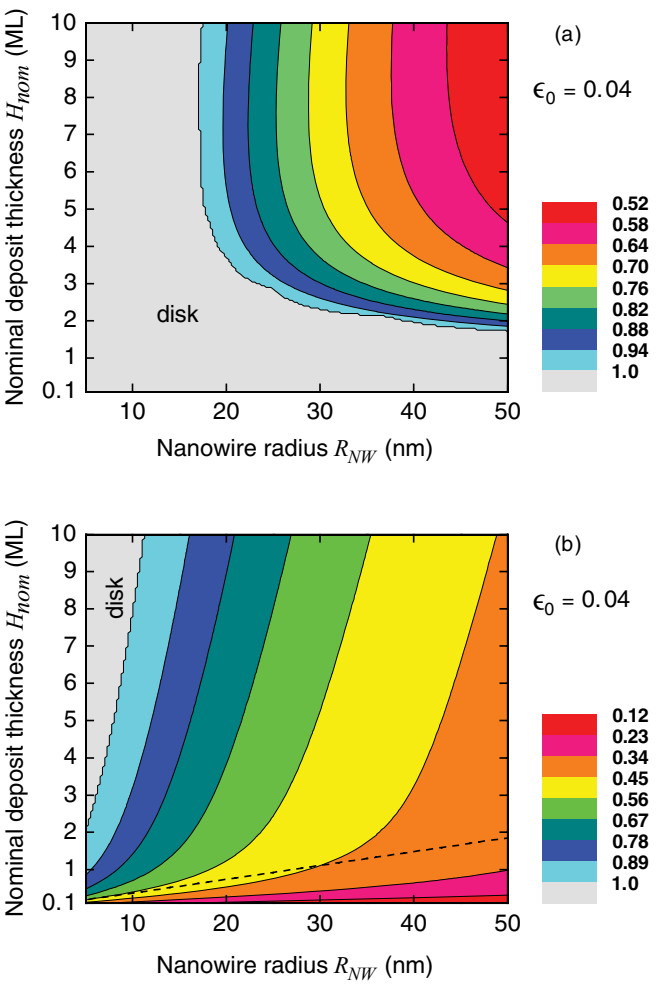

FIG. 8. (Color online) Same as Fig. 5 with nonzero differences of surface energies between the top facets of the island and NW stem: (a) $\Delta\gamma = -0.18$ J/m^2, (b) $\Delta\gamma = 0.18$ J/m^2. The dashed line in (b) marks the disk/island transition when elastic energy is ignored (see text).

towards lower values of the NW radius and deposit thickness with respect to the case $\Delta\gamma = 0$: as expected, $\Delta\gamma > 0$ favors narrow islands and ultimately true islands compared to disks. In this case also, the notion of critical radius remains pertinent, although this radius varies slightly more with deposit thickness. It is only at very low deposit thickness that the diagram is deeply modified. In particular, islands tend to form at any deposit thickness, whatever the NW radius, so that there is no longer any critical thickness. This can be understood by recalling that at small deposit thicknesses, the elastic state of the island remains quasi-2D for a wide range of radii (Fig. 6). The changes of the total energy with island radius are then mainly due to the changes of the surface energy, $W_s = 2\pi RH\gamma_{SW} + \pi R^2\Delta\gamma$. Then, at fixed island volume V,

$$\left(\frac{\partial W_s}{\partial R}\right)_V = 2\pi R\left(\Delta\gamma - \frac{V}{\pi R^3}\gamma_{SW}\right). \tag{6}$$

This shows that if $\Delta\gamma > 0$, a reduction of island radius is indeed favored when $V \to 0$, which is at variance with the case $\Delta\gamma < 0$. More precisely, based solely on surface energy, the disk becomes unstable [$(\partial W_s/\partial R)_V > 0$ for $R = R_{NW}$] if $H_{\text{nom}} < (\Delta\gamma/\gamma_{SW})\,R_{NW}$. This condition, shown as a dashed line in Fig. 8(b), correctly predicts the change of orientation of the lines of equal ratio $W_{\text{opt}}/W_{\text{disk}}$ from nearly vertical to shallowly sloped at low deposit thickness, although the quantitative determination of the critical thickness requires inclusion of the elastic energy.

It is in the case $\Delta\gamma < 0$ [Fig. 8(a)] that we may expect a true SK transition. Recall that our model only treats the complete transformation of a disk into an island and does not allow for a wetting layer coexisting with islands. Hence, for a given NW radius, the morphological transition occurs when the deposit volume becomes large enough for the energy gained in the elastic relaxation of the island to balance the increase of energy due not only to the formation of the sidewalls, but also now to the increase of the area of high energy γ_1 at the expense of the area of low energy γ_2. If the transformation preserved a wetting layer, then the gain in elastic energy would only need to compensate for the formation of the island sidewalls, and the transformation would occur at smaller deposit volumes. We would then expect a disk/island stability diagram that is intermediate between those calculated with $\Delta\gamma = 0$ (Fig. 5) and $\Delta\gamma < 0$ in the absence of a wetting layer [Fig. 8(a)].

V. DISCUSSION AND CONCLUSIONS

The main result of the present study is that islanding may considerably reduce the total energy of the system constituted of a misfitting deposit on a narrow NW stem. Whereas for low misfit the gain of energy in forming an axial island rather than a disk is null or marginal, it may become very significant at higher misfits. More generally, as in the case of growth on a bulk substrate, islanding is favored by high elastic energy (high E or high ϵ_0) and low surface energy (γ_{SW}). However, the present problem is considerably complicated by the finite width of the NW stem and, in addition to elastic constants and surface energies, there are three geometrical and structural parameters that determine the energy of the system, namely, NW radius, deposit thickness, and misfit. If one fixes the values of any two of these, then there is a critical value of the third one above which the formation of a genuine island is favored compared with that of a disk of equal volume. In addition, the critical NW radius is nearly independent of deposit thickness, except if this one is very small. This dependence of the critical values on many parameters makes it difficult to give simple criteria for islanding. However, by using our fitting functions for the elastic energy, the critical values can easily be calculated for any material system and geometry of interest.

Moreover, it is clear, from the examples given, that these critical values are easily accessible in existing NW systems. Hence, a proper choice of the relevant parameters might lead to the deterministic formation of such islands, at least in catalyst-free NW growth. We believe that spontaneous island formation has actually already been observed in NW heteroepitaxy of group-III nitrides,[29] although in the case of alloys (but, of course, not for elementary or stoichiometric binary deposits) the alternative process of inhomogeneous layer-by-layer growth [Fig. 1(a) and Ref. 30] remains a possibility. However, the observation of faceted insertions with a base narrower than the NW stem[27,29] is a strong argument in favor of island growth [Fig. 1(b)] as opposed to inhomogeneous layer-by-layer growth. These observations are no surprise since, according to our calculations (Sec. IV), even in systems where the deposit has a lower horizontal facet energy than the stem [such as (Ga,In)N on GaN[29] or GaN on AlN], which favors disks, the formation of islands is still entirely possible for realistic geometries and misfits [Fig. 8(a)].

We have determined the optimal aspect ratio of a given deposit thickness, i.e., the shape that minimizes the total energy. It might, however, be argued that due to fluctuations, when the optimal configuration is a true island ($R_{\text{opt}} < R_{NW}$), this aspect ratio might not be exactly realized. This would appear to reintroduce an element of randomness in the geometry of the deposit that is all too familiar in SK or VW growth and which would be a drawback compared to the growth of disk heterostructures that permits perfect control of the geometry of the insertion (Sec. I). However, much of the randomness in the location and the size distribution of standard SK or VW islands stems from the availability of an effectively infinite substrate for nucleation on which adatoms can diffuse, which induces a competition between neighboring nucleation sites. These factors are obviously eliminated in the case of growth on a NW stem of very limited lateral extension, on which only a small number of atoms is present, due to direct deposition and maybe due to diffusion from the sidewalls. The formation of more than one island on such a narrow stem is very unlikely and neighboring NWs could only interact via diffusion on the substrate. Moreover, after capping by a material with a larger band gap (for instance, the stem material), such islands may become quantum dots not only structurally but also as regards their electronic properties. In some systems, the capping seems to be conformal in that it also wraps the sidewalls of the island to restore the stem radius[27,29] [Fig. 1(b)]. The spontaneous formation of a lateral potential barrier is a clear advantage over the disk scheme, where a core-shell structure has to be fabricated to passivate the insertion sidewalls.

To conclude, the spontaneous formation of quantum islands on top of NWs can be considered as a quasideterministic

process with potentially beneficial aspects as regards the electronic and optical properties of NW heterostructures. The large energy gain that it affords for large enough (but perfectly reasonable) misfit, nanowire radius, and deposit thickness should make it a frequent feature of heterostructure formation, at least in catalyst-free NW growth.

ACKNOWLEDGMENTS

This work was partly carried out within Project No. BONAFO ANR-08-NANO-031 of the French Agence Nationale de la Recherche. We thank V. G. Dubrovskii, J. C. Harmand, G. Tourbot, and K. Hestroffer for fruitful discussions.

*frank.glas@lpn.cnrs.fr

[1] L. Goldstein, F. Glas, J. Y. Marzin, M. N. Charasse, and G. Le Roux, Appl. Phys. Lett. **47**, 1099 (1985).
[2] M. T. Björk, B. J. Ohlsson, C. Thelander, A. I. Persson, K. Deppert, L. R. Wallenberg, and L. Samuelson, Appl. Phys. Lett. **81**, 4458 (2002).
[3] E. D. Minot, F. Kelkensberg, M. van Kouwen, J. A. van Dam, L. P. Kouwenhoven, V. Zwiller, M. T. Borgström, O. Wunnicke, M. A. Verheijen, and E. P. A. M. Bakkers, Nano Lett. **7**, 367 (2007).
[4] M. T. Borgström, V. Zwiller, E. Müller, and A. Imamoglu, Nano Lett. **5**, 1439 (2005).
[5] A. Tribu, G. Sallen, T. Aichele, R. André, J.-P. Poizat, C. Bougerol, S. Tatarenko, and K. Kheng, Nano Lett. **8**, 4326 (2008).
[6] Y.-M. Niquet and D. Camacho Mojica, Phys. Rev. B **77**, 115316 (2008).
[7] R. Singh and G. Bester, Phys. Rev. Lett. **103**, 063601 (2009).
[8] N. Dorenbos, H. Sasakura, M. P. van Kouwen, N. Akopian, S. Adachi, N. Namekata, M. Jo, J. Motohisa, Y. Kobayashi, K. Tomioka, T. Fukui, S. Inoue, H. Kumano, C. M. Natarajan, R. H. Hadfield, T. Zijlstra, T. M. Klapwijk, V. Zwiller, and I. Suemune, Appl. Phys. Lett. **97**, 171106 (2010).
[9] J. L. Rouvière, J. Simon, N. Pelekanos, B. Daudin, and G. Feuillet, Appl. Phys. Lett. **75**, 2632 (1999).
[10] D. Dalacu, A. Kam, D. G. Austing, X. Wu, J. Lapointe, G. C. Aers, and P. J. Poole, Nanotechnology **20**, 395602 (2009).
[11] K. Hiruma, K. Tomioka, P. Mohan, L. Yang, J. Noborisaka, B. Hua, A. Hayashida, S. Fujisawa, S. Hara, J. Motohisa, and T. Fukui, J. Nanotechnol. **2012**, 169284 (2012).
[12] F. Glas, J. C. Harmand, and G. Patriarche, Phys. Rev. Lett. **99**, 146101 (2007).
[13] V. G. Dubrovskii, N. V. Sibirev, J. C. Harmand, and F. Glas, Phys. Rev. B **78**, 235301 (2008).
[14] A. D. Gamalski, C. Ducati, and S. Hofmann, J. Phys. Chem. C **115**, 4413 (2011).
[15] C.-Y. Wen, J. Tersoff, K. Hillerich, M. C. Reuter, J. H. Park, S. Kodambaka, E. A. Stach, and F. M. Ross, Phys. Rev. Lett. **107**, 025503 (2011).
[16] F. Glas, J. C. Harmand, and G. Patriarche, Phys. Rev. Lett. **104**, 135501 (2010).
[17] J.-C. Harmand, F. Glas, and G. Patriarche, Phys. Rev. B **81**, 235436 (2010).
[18] E. Ertekin, P. A. Greaney, and D. C. Chrzan, J. Appl. Phys. **97**, 114325 (2005).
[19] F. Glas, Phys. Rev. B **74**, 121302 (2006).
[20] X. Zhang, V. G. Dubrovskii, N. V. Sibirev, and X. Ren, Cryst. Growth Des. **11**, 5441 (2011).
[21] F. Glas, in *Lattice Engineering: Technologies and Applications*, edited by S. M. Wang (Pan Stanford, Singapore, 2012), Chap. 5.
[22] J.-C. Harmand, L. Liu, G. Patriarche, M. Tchernycheva, N. Akopian, U. Perinetti, and V. Zwiller, in *Conference on Quantum Sensing and Nanophotonic Devices VI, SPIE Photonics West 2009*, Proc. SPIE, Vol. 7222, edited by M. Razeghi, R. Sudharsanan, and G. J. Brown (The International Society for Optical Engineering, Bellingham, WA, 2009), p. 722219.
[23] M. Den Hertog, M. Elouneg-Jamroz, E. Bellet-Amalric, S. Bounouar, C. Bougerol, R. André, Y. Genuist, J. P. Poizat, K. Kheng, and S. Tatarenko, J. Appl. Phys. **110**, 034318 (2011).
[24] J. Renard, R. Songmuang, G. Tourbot, C. Bougerol, B. Daudin, and B. Gayral, Phys. Rev. B **80**, 121305 (2009).
[25] L. Rigutti, G. Jacopin, A. De Luna Bugallo, M. Tchernycheva, E. Warde, F. H. Julien, R. Songmuang, E. Galopin, L. Largeau, and J.-C. Harmand, Nanotechnology **21**, 425206 (2010).
[26] F. Furtmayr, J. Teubert, P. Becker, S. Conesa-Boj, J. R. Morante, A. Chernikov, S. Schäfer, S. Chatterjee, J. Arbiol, and M. Eickhoff, Phys. Rev. B **84**, 205303 (2011).
[27] Y.-L. Chang, J. L. Wang, F. Li, and Z. Mia, Appl. Phys. Lett. **96**, 013106 (2010).
[28] G. Tourbot, C. Bougerol, A. Grenier, M. Den Hertog, D. Sam-Giao, D. Cooper, P. Gilet, B. Gayral, and B. Daudin, Nanotechnology **22**, 075601 (2011).
[29] G. Tourbot, C. Bougerol, F. Glas, L. F. Zagonel, Z. Mahfoud, S. Meuret, P. Gilet, M. Kociak, B. Gayral, and B. Daudin, Nanotechnology **23**, 135703 (2012).
[30] X. Niu, G. B. Stringfellow, and F. Liu, Phys. Rev. B **85**, 165316 (2012).
[31] L. Pan, K.-K. Lew, J. M. Redwing, and E. C. Dickey, Nano Lett. **5**, 1081 (2005).
[32] E. Uccelli, J. Arbiol, J. R. Morante, and A. Fontcuberta i Morral, ACS Nano **4**, 5985 (2010).
[33] X. Yan, X. Zhang, X. Ren, J. Li, X. Lv, Q. Wang, and Y. Huang, Appl. Phys. Lett. **101**, 023106 (2012).
[34] V. Schmidt, P. C. McIntyre, and U. Gösele, Phys. Rev. B **77**, 235302 (2008).
[35] For detailed documentation, see COMSOL website, http://www.comsol.com/
[36] K. Nakajima, T. Ujihara, G. Sazaki, and N. Usami, J. Cryst. Growth **220**, 413 (2000).
[37] K. Nakajima, T. Ujihara, S. Miyashita, and G. Sazaki, J. Appl. Phys. **89**, 146 (2001).
[38] K. Rapcewicz, B. Chen, B. Yakobson, and J. Bernholc, Phys. Rev. B **57**, 7281 (1998).
[39] S.-M. Ko, J.-H. Kim, Y.-H. Ko, Y. H. Chang, Y.-H. Kim, J. Yoon, J. Y. Lee, and Y.-H. Cho, Cryst. Growth Des. **12**, 3838 (2012).
[40] J. E. Northrup and J. Neugebauer, Phys. Rev. B **53**, R10477 (1996).
[41] A. Filippetti, V. Fiorentini, G. Cappellini, and A. Bosin, Phys. Rev. B **59**, 8026 (1999).